

MODELING FRACTURE POPULATIONS IN EUROPA'S BRITTLE ICE SHELL AND IMPLICATIONS OF FRACTURE-ADDED POROSITY. C. A. Mondro¹, J. Emery², and J. E. Moersch¹. ¹Department of Earth and Planetary Sciences, University of Tennessee, Knoxville, Tennessee 37996-1526, USA (cmondro@vols.utk.edu), ²Department of Astronomy and Planetary Sciences, Northern Arizona University, Flagstaff, AZ 86011-6020.

Introduction: Many current models of Europa ice shell evolution and formation of features such as chaos terrain require movement and short-term storage of melt within the outer brittle layer of ice [1–3]. Some melt movement within the ice shell can be explained by thermal convection, but matrix porosity and open fractures can also act as pathways and storage space for liquid melt [4–6].

Models and predictions for Europa's ice shell porosity vary wildly. Estimates based primarily on ice rheology models, which are not well constrained, range from 5% [4] to 35% [7,8]. These estimates do not include localized fracture porosity as an individual component but rather estimate the total average porosity of the ice shell. Fracture populations add to the effective porosity of a material, increasing the volume of space available for accumulation, and increase the effective permeability.

Tensile fracture populations in brittle material are self-organizing and generally follow a common distribution [9], in which the length and frequency of smaller fractures occurring between the highest-order fractures reliably follow a power-law distribution [10–12]. Therefore, a full fracture population can be modeled from the set of largest fractures present.

Large fractures are detectable in Galileo images of Europa's surface (Figure 1). In Europa's shell, fractures would be constrained to the outer brittle layer [8], estimated to be about 2 km thick [13]. Based on what is known about fracture populations in brittle material on Earth, we hypothesize that these large fractures are only a portion of the total fracture population within the brittle layer of Europa's ice shell and that a full distribution of smaller fractures exists below the limit of resolution of the current image data.

Objectives: We calculate a potential fracture population based on standard patterns of extensional fracture behavior and the dimensions of large fractures in Europa's brittle ice shell and use the modeled fracture population to calculate fracture-added porosity. This project presents preliminary data that will be further refined and expanded upon in ongoing work. Our goal is to use these estimates as a starting point to discuss the potential for enhanced fluid flow and melt storage in Europa's outer ice layer due to fracture-added porosity and permeability.

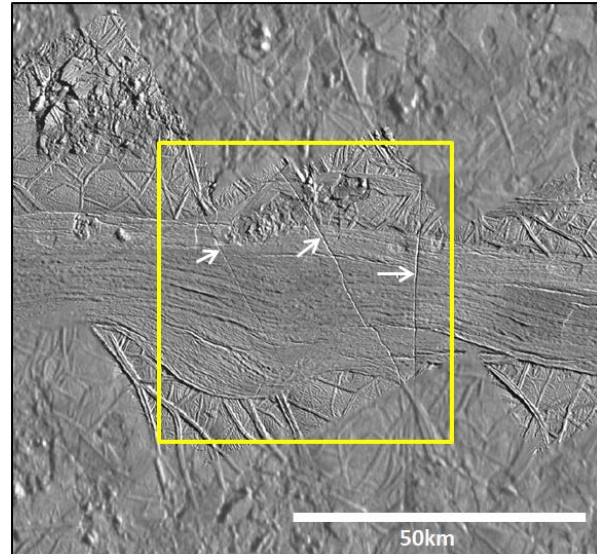


Figure 1. Galileo image PIA01646 showing three large tension fractures which were used as basis for fracture population calculation. Fractures are estimated to be approximately 50 m in length with an average aperture of 100 m. The yellow square designates total ice volume encompassing modeled fracture population. Image credit: NASA/JPL

Methods: We modeled a standard fracture population based on a power law frequency distribution

$$N(l) = \alpha l^{-(a-1)} dl$$

where $N(l)$ is the number of fractures within each length bin l and α is the density constant [10]. The exponent a defines the distribution of the fracture population. It depends on material properties and is typically between 1.0 and 3.2 [10]. For this calculation, bin size was chosen to follow a logarithmic progression and therefore the exponent of the equation equals $(a-1)$. We based the fracture population on an observable set of three large fractures on Europa (Figure 1) and calculated α to fit the distribution to the approximate size of the largest observable fractures, using $a = 3.0$.

We calculated total fracture volume from the volume of the average fracture in each length bin multiplied by the modeled $N(l)$ fracture frequency. Because fractures in Europa's outer ice shell would be constrained to the brittle layer [8], we assume that all

fractures with $l > 2$ km terminate at 2 km depth and that fractures of $l < 2$ km terminate at depth = l . Fracture aperture is defined as the width of the fracture opening measured perpendicular to the fracture plane and fracture opening is defined as the percent of the fracture that acts as open pore space. Fractures that have been partially filled can be represented by a smaller fracture opening value. For this simulation we use a linear aperture to length relationship and assume a fracture opening of 100%, where the full volume of the fracture acts as pore space. This is an end-member case which can be further refined in subsequent work. Total ice porosity is calculated by $l_{max} \times l_{max} \times 2$ km to represent the volume of the ice shell estimated to contain this fracture set.

Results and Discussion: The calculated fracture population distribution has $l_{max} = 50$ km and $l_{min} = 10$ m and fits a standard power law frequency distribution of $(a-1) = 2$ (Figure 2). Total calculated fracture volume is 9.0×10^{10} m³ and total ice volume is estimated as 5.0×10^{12} m³, producing a total fracture-added porosity of 1.8% for this particular modeled fracture population.

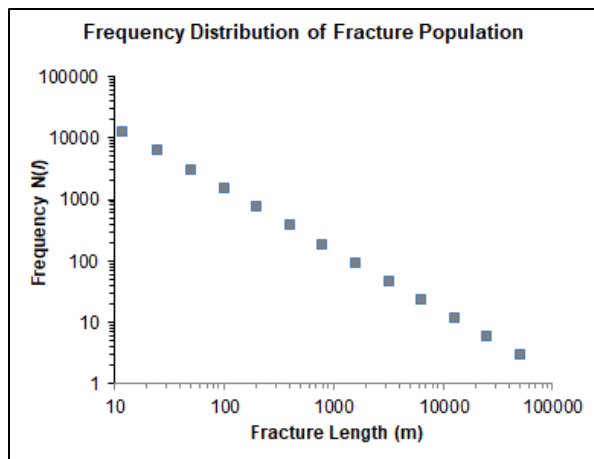


Figure 2. Number of calculated fractures within each length bin based on a power law frequency distribution. The modeled population has been fit to the largest observed fractures from Figure 1 so that $N(50000) = 3$.

This fracture population includes a total of 25,072 fractures, nearly all of which are below the limit of resolution of currently available 50 m/pixel Galileo image data from Europa. Higher resolution image data acquired by the Europa Clipper mission will help identify smaller fractures with which we will be able to further refine fracture population models.

As a part of our ongoing work, we plan to expand upon this initial model by further refining the a and α

values used in the frequency distribution calculation based on more specific estimates of Europa's ice shell tensile strength and regional variations in observed fracture density. This initial fracture population model was made to fit a distribution that would include three large fractures, as observed in Figure 1, but can also be adapted to fit other observed or hypothesized fracture populations. In addition, we plan to use this initial model as a starting point to calculate a range of fracture-added porosity values from varying length-aperture ratios and length-depth ratios that may be present.

Because porosity of the ice shell affects models of the mechanics of tidal flexure [5] and rotational dynamics [14], it is critical to have accurate and reasonable values of porosity as model parameters. There is also the possibility that by not accounting for fracture-added porosity, the current models of fluid interaction with the ice shell are significantly underestimating the availability of fluid migration pathways in localized, highly fractured areas. We suggest that fracture-added porosity can be modeled even where it cannot be measured or estimated directly from remote sensing data and that including it in ice shell models will further refine our understanding of surface feature formation.

References: [1] Collins, G. and Nimmo, F. (2009) *Europa, The University of Arizona Space*, 259–281. [2] Doggett, T., et al. (1999) *Geologic Stratigraphy and Evolution of Europa's Surface*, 137–159. [3] Schmidt, B.E., et al. (2011) *Nature*, 479 (7374), 502–505. [4] Craft, K.L., et al. (2016) *Icarus*, 274 297–313. [5] Rudolph, M. L. and Manga, M. (2009) *Icarus*, 199 (2), 536–541. [6] Kalousová, K., et al. (2014) *JGR: Planets*, 119 (3), 532–549. [7] Schmidt, B. E., et al. (2011) *Nature*, 479 (7374), 502–505. [8] Lee, S., et al. (2005) *Icarus*, 177 (2), 367–379. [9] Schultz, R. A., et al. (2010) *Planetary Tectonics*, Cambridge University Press. [10] Bonnet, E., et al. (2001) *Reviews of Geophysics*, 39 (3), 347–383. [11] Pickering, G., et al. (1995) *Tectonophysics*, 248 (1–2), 1–20. [12] Rist, M. A., et al. (1999) *JGR: Solid Earth*, 104 (B2), 2973–2987. [13] Pappalardo, R. T., et al. (1999) *JGR*, 104 (E10), 24,015–24,055. [14] Nimmo, F. and Manga, M. (2009) *Europa Univ. Arizona*, pp. 381–404.